Chapter 18
Light Forces

Abstract In recent years it has become possible to manipulate atoms with light beams, to trap them and cool them to temperatures of milliKelvin and below. The first proposal of laser cooling by Hänsch and Schawlow [1] was based upon Doppler cooling in a two-level atom. Consider an atom irradiated by counterpropagating laser beams tuned to the low frequency side of atomic resonance. The beam counter-propagating with the atom will be Doppler shifted towards resonance, thus increasing the probability of photon absorption. The beam co-propagating with the atom will be frequency-shifted away from resonance, so there will be a net absorption of photons opposing the motion of the atom. The absorbed photon gives the atom a momentum impulse $\Delta p = \hbar k = h/\lambda$ in the direction of the beam. The atom re-emits a photon by spontaneous emission in a random scattering direction. Thus, the net force of the time averaged emitted photons is zero. The resultant force due to the absorption of the photons opposes the atom's motion. By surrounding the atom with three pairs of counter-propagating beams along the x, y and z axes, a drag force opposing the velocity of the atom can be generated. The term "optical molasses" was coined to describe this situation. For two level atoms the minimum temperature achievable, the so-called Doppler limit, was predicted to be $k_B T = \hbar\gamma/2$, where γ is the atomic decay rate. Optical molasses in sodium was first observed in 1985 by *Chu* et al. [2] with a temperature $\sim 240\,\mu$K, close to the Doppler limit.

In order to trap the cold atoms, techniques including purely optical forces, the dipole trap, or a combination of optical and magnetic forces, the magneto-optical trap (MOT), were developed. Experiments performed by W. Phillips [3] and colleagues cooling sodium atoms in a MOT recorded temperatures considerably lower than expected, i.e. $\sim 40\,\mu$K as opposed to $T_D \sim 240\,\mu$K. The explanation for the lower temperatures observed experimentally was given by *Dalibard* and *Cohen-Tannoudji* [4] and *Chu* [5] and colleagues. They showed that optical pumping between atomic magnetic sublevels could result in lower temperatures (sub-Doppler cooling) with a limit close to the recoil energy,

$$k_B T = \hbar\omega_{\mathrm{Rec}} ,$$

with $\hbar\omega_{\mathrm{Rec}} = \hbar^2 k^2/2M$.

More recently, sub recoil cooling schemes have been proposed and implemented, using, for example, the accumulation of ultracold atoms in dark states, which do not couple to the light fields provided the atomic kinetic energy is less than the recoil energy.

In 1997 the Nobel Prize in Physics was awarded to Steven Chu, Claude Cohen-Tannoudji and William Phillips for their work on atom trapping and cooling. In this chapter we shall present a theoretical description of light forces on a two level atoms. We shall follow closely the treatment developed by *Gordon* and *Ashkin* [6] and *Cohen-Tannoudji* [7].

18.1 Radiative Forces in the Semiclassical Limit

We begin with the Hamiltonian for a two–level atom coupled to the electromagnetic field and driven by a near–resonant laser field:

$$\mathscr{H} = \mathscr{H}_{\rm A} + \mathscr{H}_{\rm V} + \mathscr{H}_{\rm AL} + \mathscr{H}_{\rm AV} \,. \tag{18.1}$$

Here, $\mathscr{H}_{\rm A}$ is the atomic Hamiltonian,

$$\mathscr{H}_{\rm A} = \frac{\vec{P}^2}{2m} + \frac{\hbar\omega_a}{2}\sigma_z \tag{18.2}$$

with $\sigma_z = (|e\rangle\langle e| - |g\rangle\langle g|)$, $\mathscr{H}_{\rm V}$ is the Hamiltonian of the (vacuum) radiation field, $\mathscr{H}_{\rm AV}$ is the coupling of the atom to this field, and $\mathscr{H}_{\rm AL}$ describes the atom–laser coupling,

$$\mathscr{H}_{\rm AL}(\vec{R}) = -\vec{d}\cdot\vec{E}_{\rm L}(\vec{R},t) = \hbar\Omega_{\rm L}(\vec{R})\left[\sigma_+ {\rm e}^{-{\rm i}(\omega_{\rm L}t-\Phi(\vec{R}))} + {\rm h.c.}\right] \,, \tag{18.3}$$

where $\sigma_+ = |e\rangle\langle g|$ and the rotating wave approximation has been made. The interaction with the vacuum field is

$$\mathscr{H}_{\rm AV}(\vec{R}) = \hbar\left[\sigma_+\Gamma(\vec{R}) + \sigma_-\Gamma^\dagger(\vec{R})\right] \,, \tag{18.4}$$

where $\Gamma(\vec{R})$ is the bath operator for the vacuum defined as

$$\Gamma(\vec{R}) = \sum_k g_k b_k {\rm e}^{-{\rm i}(\omega_k t - \vec{k}\cdot\vec{R})} \tag{18.5}$$

(see Sect. 10.1).

The force acting, $\vec{F}(\vec{R})$, on the atom is given by

$$\vec{F}(\vec{R}) = -\nabla\mathscr{H}_{\rm AL}(\vec{R}) - \nabla\mathscr{H}_{\rm AV}(\vec{R})$$

The coupling of the atom to the vacuum radiation field is responsible for spontaneous emission. This process introduces friction and damping to the system–necessary for Doppler cooling – but it also introduces some of the fluctuations which lead to momentum diffusion, limiting the final temperatures.

In a classical description the atom has a well–defined position and a well–defined momentum. For a semiclassical description to be valid, one therefore requires that the atomic wave packet be sufficiently well localised in position space and in momentum space.

Denote the spatial and momentum spreads of the atomic wave packet by ΔR and ΔP, which must satisfy $(\Delta R)(\Delta P) \geq \hbar$. The force exerted by the laser on the atom varies on a distance determined by the laser wavelength λ_L. If the atom is very well localised on this scale we can neglect the fluctuations of the force due to the spread in atom positions and simply evaluate the force at the average position of the wave packet. Furthermore, as atoms moving with different velocities see a varying Doppler shift, the force due to the laser will also fluctuate due to momentum fluctuations. However if the initial momentum fluctuations are small enough we can neglect fluctuations in Doppler shifts and assume all atoms see a single Doppler shift determined by the mean velocity of the atomic wave packet. We are thus led to two conditions for a semiclassical description to be valid (i) that the position spread be small compared to λ_L,

$$\Delta R \ll \lambda_L \quad \Leftrightarrow \quad k_L \Delta R \ll 1 \tag{18.6}$$

and
(ii) that the velocity spread be small enough that the corresponding spread of Doppler shifts be negligible compared to the natural linewidth γ,

$$\frac{k_L \Delta P}{m} \ll \gamma \,. \tag{18.7}$$

Combining (18.6) and (18.7) with the uncertainty relation gives

$$\frac{\hbar k_L^2}{m} \ll \gamma \quad \text{or} \quad \hbar\omega_{\text{rec}} \ll \hbar\gamma \,. \tag{18.8}$$

It turns out that this is equivalent to the condition that the timescale for internal atomic evolution ($\sim \gamma^{-1}$) is much shorter than the timescale for external evolution [$\sim (\hbar k_L^2/m)^{-1}$], i.e., for damping of the motion.

We now denote the *mean* atomic position and momentum by $\vec{r} = \langle \vec{R} \rangle$ and $\vec{p} = \langle \vec{P} \rangle$. The semiclassical force is given by

$$\vec{f} = -\left\langle \nabla \mathscr{H}_{\text{AL}}(\vec{r},t) \right\rangle|_{\vec{r}=\vec{r}_0+\vec{v}_0 t} \,. \tag{18.9}$$

Note that contribution from the atom–vacuum–field coupling term, $\mathscr{H}_{\text{AV}}$, vanishes, due to the symmetry of spontaneous emission. Now

$$-\nabla \mathscr{H}_{\text{AL}}(\vec{r},t) = -\hbar\,\sigma_+ \exp^{-\mathrm{i}\omega_L t} \nabla \left[\Omega(\vec{r}) \exp^{-\mathrm{i}\Phi(\vec{r})} \right] + \text{h.c.}\,, \tag{18.10}$$

and we can write

$$\nabla\left[\Omega_{\rm L}(\vec{r})\exp^{-{\rm i}\Phi(\vec{r})}\right] = \Omega_{\rm L}(\vec{r})\exp^{-{\rm i}\Phi(\vec{r})}\left[\vec{\alpha}(\vec{r}) - {\rm i}\vec{\beta}(\vec{r})\right] \tag{18.11}$$

where

$$\vec{\alpha}(\vec{r}) = \frac{\nabla\Omega_{\rm L}(\vec{r})}{\Omega_{\rm L}(\vec{r})}\,, \quad \vec{\beta}(\vec{r}) = \nabla\Phi(\vec{r})\,. \tag{18.12}$$

$\vec{\alpha}(\vec{r})$ – characterises spatial variation of the Rabi frequency.

$\vec{\beta}(\vec{r})$ – characterises spatial variation of the phase.

This gives the following expression for the mean force,

$$\begin{aligned}\vec{f}(\vec{r},t) &= -2{\rm Re}\left\{\langle\sigma_+(t)\rangle\,\hbar\Omega_{\rm L}(\vec{r})\exp^{-{\rm i}[\omega_{\rm L}t+\Phi(\vec{r})]}\left[\vec{\alpha}(\vec{r}) - {\rm i}\vec{\beta}(\vec{r})\right]\right\} \\ &= -2\hbar\Omega_{\rm L}(\vec{r})\left[u(t)\vec{\alpha}(\vec{r}) + v(t)\vec{\beta}(\vec{r})\right]\,,\end{aligned} \tag{18.13}$$

where $\langle\sigma_+(t)\rangle = {\rm Tr}[\sigma_+\rho_{\rm int}(t)]$, with $\rho_{\rm int}(t)$ the internal atomic density operator, and

$$u(t) = {\rm Re}\left\{\langle\sigma^+(t)\rangle\exp^{-{\rm i}[\omega_{\rm L}t+\Phi(\vec{r})]}\right\} \tag{18.14}$$

$$v(t) = {\rm Im}\left\{\langle\sigma^+(t)\rangle\exp^{-{\rm i}[\omega_{\rm L}t+\Phi(\vec{r})]}\right\}\,. \tag{18.15}$$

The average values of the internal atomic operators are computed from the optical Bloch equations, which, in terms of the variables defined above, take the form

$$\begin{aligned}\dot{u} &= -(\gamma/2)u + (\delta+\dot{\Phi})v \\ \dot{v} &= -(\gamma/2)v - (\delta+\dot{\Phi})u - 2\Omega_{\rm L}w \\ \dot{w} &= -(\gamma/2) - \gamma w + 2\Omega_{\rm L}v\end{aligned} \tag{18.16}$$

where $w = [\langle\sigma^+\sigma^-\rangle - \langle\sigma^-\sigma^+\rangle]/2$ is the inversion, $\delta = \omega_{\rm L} - \omega_{\rm A}$ is the laser–atom detuning, and

$$\dot{\Phi} = \vec{v}\cdot\nabla\Phi = \vec{v}\cdot\beta\,. \tag{18.17}$$

18.2 Mean Force for a Two–Level Atom Initially at Rest

Some physical insight into the nature of the forces acting on the atom can be gained by considering the zero velocity case. Consider a two–level atom initially at rest at the origin:

$$\vec{r} = 0\,, \quad \vec{p} = 0\,. \tag{18.18}$$

The steady state solutions of the optical Bloch equations are:

$$u_{\rm ss} = \frac{\delta}{2\Omega_{\rm L}} \frac{s}{1+s} \tag{18.19}$$

$$v_{\rm ss} = \frac{\gamma}{4\Omega_{\rm L}} \frac{s}{1+s} \tag{18.20}$$

$$w_{\rm ss} = -\frac{1}{2(1+s)} \tag{18.21}$$

where s is the saturation parameter,

$$s = \frac{2\Omega_{\rm L}^2}{\delta^2 + (\gamma^2/4)} \,. \tag{18.22}$$

Note that the population of the upper state is given by

$$P_{\rm ss}^e = w_{\rm ss} + 1/2 = \frac{1}{2} \frac{s}{1+s} \,. \tag{18.23}$$

Substituting the steady-state values $u_{\rm ss}$ and $v_{\rm ss}$ in the expression (18.13) for the force gives the average force in the case where the internal degrees of freedom have reached their steady state (adiabatic approximation). The mean force $\vec{f}f$ is the sum of two contributions proportional to v and u, respectively. These two contributions are known as the *spontaneous force* and the *dipole force* (or *dissipative force* and *reactive force*).

The spontaneous force is due to the radiation pressure. It results from the absorption of photons from a traveling wave laser from which the atom receives a transfer of momentum. The subsequent spontaneous emission of photons does not contribute to the average force since spontaneous emission occurs with equal probabilities in all directions. The dissipative force is zero for a stationary atom in a standing wave since absorption of photons from both directions cancel. The spontaneous force is given by the component proportional to $v_{\rm ss}$,

$$\vec{f}_{\rm spon} = -2\hbar\Omega_{\rm L} v_{\rm ss} \vec{\beta} \,. \tag{18.24}$$

Note that $-2\Omega_{\rm L} v_{\rm ss} = \gamma \rho_{\rm ss}^e$ which is simply the mean number of photons spontaneously emitted per unit time.

For a plane wave,

$$\vec{E}_L(\vec{r},t) = \vec{E}_0 \cos\left(\omega t - \vec{k}_{\rm L} \cdot \vec{R}\right) \tag{18.25}$$

The phase of the field is $\Phi(\vec{r}) = -\vec{k}_{\rm L} \cdot \vec{R}$ which gives

$$\beta = \nabla\Phi|_{\vec{r}=0} = -\vec{k}_{\rm L} \,, \tag{18.26}$$

and the force,

$$f_{\text{spon}} = \hbar k_{\text{L}} \left(\frac{\gamma}{2}\right) \frac{2\Omega_{\text{L}}^2}{\delta^2 + \dfrac{\gamma^2}{4} + 2\Omega_{\text{L}}^2} \,. \tag{18.27}$$

For low intensity ($s \ll 1$) $f_{\text{spon}} \propto \Omega_{\text{L}}^2 \sim I_{\text{L}}$ (laser intensity). For high intensity laser fields $f_{\text{spon}} \to \hbar k_{\text{L}} \frac{\gamma}{2}$, that is the maximum force is limited by the spontaneous emission rate. The maximum acceleration imparted to the atom by the dissipative force is,

$$\vec{a}_{\text{max}} = \frac{\hbar \vec{k}_{\text{L}}}{m} \frac{\gamma}{2} \,. \tag{18.28}$$

While the recoil velocity $v_{\text{recoil}} = \frac{\hbar k_{\text{L}}}{m}$ due to absorption of a single photon is small ($\sim$3 cm/sec for sodium, $\sim$3 mm/sec for cesium), the number of fluorescent cycles/sec is high for intense fields. For sodium $\gamma^{-1} = 1.6 \times 10^{-8}$ s, which gives $a_{\text{max}} \sim 10^6$ m/s^2 which is 10^5 times the acceleration due to gravity.

The dipole force is given by the component proportional to u_{ss}:

$$\vec{f}_{\text{dip}} = -2\hbar\Omega_{\text{L}} u_{\text{ss}} \vec{\alpha} \tag{18.29}$$

In a plane travelling wave, $\vec{\alpha} = 0$ as the amplitude is independent of $\vec{r}$ and hence $\vec{f}_{\text{dip}} = 0$. The dipole force is only nonzero if the laser field is a superposition of plane waves, e.g., a *laser standing wave*. The dipole force results from the absorption of a photon with momentum $\hbar k$ from a standing wave and reemission of a photon in the opposite direction, that is with momentum $-k$. This results in a total momentum gain for the atom $2\hbar k$. For a travelling wave laser the dipole force is zero since photons can only be reemitted into the same direction from which they where absorbed.

Using the solution for u_{ss},

$$\vec{f}_{\text{dip}} = -\hbar\delta \frac{\nabla(\Omega_{\text{L}}^2)}{\delta^2 + (\gamma^2/4) + 2\Omega_{\text{L}}^2} \tag{18.30}$$

For $\delta < 0$ ($\omega_{\text{L}} < \omega_{\text{A}}$), the dipole force pushes the atom towards regions of higher intensity since $\text{sgn}\{\vec{f}_{\text{dip}}\} = \text{sgn}\{\nabla I_{\text{L}}\}$ (and vice–versa for $\delta > 0$). For each value of Ω_{L}^2 (with $\Omega_{\text{L}} \gg \gamma$), $\vec{f}_{\text{dip}}$ is optimised for $\delta \sim \Omega_{\text{L}}$, and

$$\left(\vec{f}_{\text{dip}}\right)_{\text{max}} \simeq \frac{\hbar\nabla(\Omega_{\text{L}}^2)}{\Omega_{\text{L}}} \simeq \hbar\nabla\Omega_{\text{L}} \tag{18.31}$$

Hence, $\vec{f}_{\text{dip}}$ increases with laser intensity and is not bounded like $\vec{f}_{\text{spon}}$ so that much greater acceleration is possible with the dipole force.

The dipole force can be derived from an effective potential U as

$$\vec{F}_{\text{dip}} = -\nabla U \,, \tag{18.32}$$

with

$$U(\vec{r}) = \frac{\hbar\delta}{2} \ln\left[1 + \frac{2\Omega_{\mathrm{L}}^2(\vec{r})}{\delta^2 + (\gamma^2/4)}\right] . \tag{18.33}$$

For $\delta < 0$, a region of maximum intensity appears as an attractive *potential well* for the atom. For a given Ω_{L}, the maximum depth of the potential well occurs for a saturation parameter $s \simeq 4$ giving

$$|U_{\max}| \simeq 0.6\,|\hbar\Omega_{\mathrm{L}}^{\max}| . \tag{18.34}$$

18.3 Friction Force for a Moving Atom

Now suppose that the atom is moving with a velocity $\vec{v}$, such that

$$\vec{r} = \vec{v}t \quad (\vec{r} = 0 \text{ at } t = 0) . \tag{18.35}$$

As previously we assume also that we are in the semiclassical limit so that fluctuations in velocity due to momentum dispersion in the wave packet can be ignored. The velocity, $\vec{v}$, is determined by the average momentum of the wave packet. We assume a laser plane wave with wave vector $\vec{k}_{\mathrm{L}}$, so that the Rabi frequency

$$\Omega_{\mathrm{L}}(\vec{r} = \vec{v}t) = \Omega_0 = \text{ constant} \tag{18.36}$$

while

$$\Phi(\vec{r}) = -\vec{k}_{\mathrm{L}} \cdot \vec{r} \quad \Rightarrow \quad \dot{\Phi} = \frac{\mathrm{d}\vec{r}}{\mathrm{d}t} \cdot \nabla\Phi = \vec{v} \cdot \nabla\Phi = -\vec{k}_{\mathrm{L}} \cdot \vec{v} . \tag{18.37}$$

Since Ω_{L} and $\dot{\Phi}$ are time independent (and hence the coefficients of the optical Bloch equations are time independent), the steady state solutions are as before (for a stationary atom), but with $\omega_{\mathrm{L}} \to \omega_{\mathrm{L}} - \vec{k}_{\mathrm{L}} \cdot \vec{v}$, i.e., an atom moving with velocity $\vec{v}$ "sees" the laser frequency shifted by the *Doppler shift* $-\vec{k}_{\mathrm{L}} \cdot \vec{v}$. Hence, the force is

$$\vec{f} = \hbar\vec{k}_{\mathrm{L}} \frac{\gamma}{2} \frac{2\Omega_0^2}{(\delta - \vec{k}_{\mathrm{L}} \cdot \vec{v})^2 + (\gamma^2/4) + 2\Omega_0^2} . \tag{18.38}$$

We assume $\vec{k}_{\mathrm{L}} = -k_{\mathrm{L}}\vec{e}_x$ and consider motion along the x axis. For $\delta < 0$ (and $v_x > 0$), the force is negative and has a maximum where $\delta = -k_{\mathrm{L}}v_x$, i.e., where the apparent laser frequency $\omega_{\mathrm{L}} + k_{\mathrm{L}}v_x = \omega_{\mathrm{A}}$ (see Fig. 18.1). Near $v_x = 0$, one can make an expansion in the velocity, writing where the term linear in v_x is a friction force, since it is proportional to v_x. The coefficient of proportionality, α, is called the *friction coefficient* and is derived as

$$\alpha = -\hbar k_{\mathrm{L}}^2 \frac{s}{(1+s)^2} \left(\frac{\delta\gamma}{\delta^2 + (\gamma^2/4)}\right) \tag{18.39}$$

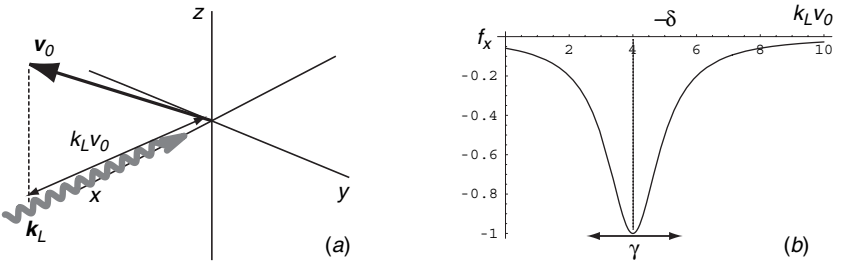

Fig. 18.1 (a) Atom moving with velocity v_0 in a laser travelling wave with wave vector $\vec{k}_{\rm L}$. (**b**) Mean force experienced by the atom versus $k_{\rm L}v_0$ in units of $\hbar k_{\rm L}\gamma$

where $s = (2\Omega_0^2)/[\delta^2 + (\gamma^2/4)]$. The friction coefficient is optimised for $\delta = -\gamma/2$ and $s = 1$ ($\Omega_0 = \gamma/2$), giving

$$\alpha_{\max} = \frac{\hbar k_{\rm L}^2}{4}\,, \tag{18.40}$$

so that the atomic velocity is damped at a rate

$$\frac{\alpha}{m} = \frac{\hbar k_{\rm L}^2}{4m} = \frac{\varepsilon_{\rm rec}}{2\hbar} \tag{18.41}$$

where $\varepsilon_{\rm rec}$ is the recoil energy, i.e., the external atomic variables, such as the velocity, have a characteristic damping time on the order of $\hbar/\varepsilon_{\rm rec}$ (typically between $1 - 100\,\mu{\rm s} \gg \gamma^{-1}$).

18.3.1 Laser Standing Wave—Doppler Cooling

The interaction with a standing wave can be considered as the interaction with a superposition of two counter-propagating plane waves with the same amplitude E_0. However the force exerted by the two standing waves is not just the sum of the radiation pressures of the two counter-propagating plane waves. Interference terms play an important role.

We now consider a laser standing wave along the x axis, linearly polarised along the z axis, so that

$$\begin{aligned}\vec{E}_{\rm L}(\vec{r},t) &= \vec{\varepsilon}_z \mathscr{E}_0 \left[\cos(\omega_{\rm L}t - k_{\rm L}x) + \cos(\omega_{\rm L}t + k_{\rm L}x)\right] \\ &= 2\vec{\varepsilon}_z \mathscr{E}_0 \cos(k_{\rm L}x)\cos(\omega_{\rm L}t)\end{aligned} \tag{18.42}$$

The phase of the field is the same everywhere ($\vec{\beta} = 0$), while the Rabi frequency is position dependent and can be written

$$\Omega_{\rm L}(x) = 2\Omega_0 \cos(k_{\rm L}x) \tag{18.43}$$

where $\Omega_0 = -(d\mathscr{E}_0)/(2\hbar)$, and

$$\vec{\alpha} = -k_{\rm L} \tan(k_{\rm L} x)\vec{\varepsilon}_x \,. \tag{18.44}$$

For a moving atom, one can replace x with $v_x t$ in the optical Bloch equations, then $\Omega_{\rm L}(x)$ becomes a sinusoidal function of t. In general, it is impossible to solve these equations analytically.

For small velocities we can use an approximation scheme, first introduced by *Gordon* and *Ashkin* [6], in which one makes an expansion in powers of $k_{\rm L} v_x/\gamma$. The zeroth order term represents the "adiabatic" solution, corresponding to the situation where the motion is so slow that the internal state of an atom passing the position x is the same as if it were at rest at x. The first order term gives the first correction to the adiabatic approximation. Note that $k_{\rm L} v_x/\gamma$ is equal to the ratio between the distance $v_x \gamma^{-1}$ over which the atom travels during the internal response time γ^{-1} and the laser wavelength k^{-1}.

The expansion proceeds as follows. We write

$$\dot{\mathbf{u}} = \left(\frac{\partial}{\partial t} + v\frac{\partial}{\partial x}\right)\mathbf{u} = \mathscr{B}\mathbf{u} - \mathbf{s} \tag{18.45}$$

where

$$\mathbf{u} = \begin{pmatrix} u \\ v \\ w \end{pmatrix} \,, \quad \mathbf{s} = \begin{pmatrix} 0 \\ 0 \\ \gamma/2 \end{pmatrix} \,, \quad \mathscr{B} = \begin{bmatrix} -\gamma/2 & \delta & 0 \\ -\delta & -\gamma/2 & -2\Omega_{\rm L}(x) \\ 0 & 2\Omega_{\rm L}(x) & -\gamma \end{bmatrix} \tag{18.46}$$

and the "hydrodynamic derivative" $\mathrm{d}/\mathrm{d}t = (\partial/\partial t) + v_x(\partial/\partial x)$ has been used. In the steady state, we write

$$v\frac{\partial}{\partial x}\mathbf{u} = \mathscr{B}\mathbf{u} - \mathbf{s} \tag{18.47}$$

and insert the expansion

$$\mathbf{u} = \mathbf{u}^{(0)} + \mathbf{u}^{(1)} + \ldots \tag{18.48}$$

of $\mathbf{u}$ in powers of $k_{\rm L} v_x/\gamma$. To order 0,

$$\mathbf{u}^{(0)} = \mathscr{B}^{-1}\mathbf{s} \,, \tag{18.49}$$

which is the steady state Bloch vector for an atom at rest in x. To order 1, we get

$$v\frac{\partial}{\partial x}\mathbf{u}^{(0)} = \mathscr{B}\mathbf{u}^{(1)} \quad \Rightarrow \quad \mathbf{u}^{(1)} = \mathscr{B}^{-1} v\frac{\partial}{\partial x}\mathbf{u}^{(0)} \,. \tag{18.50}$$

Inserting the expansion for u into the expression for the force, one obtains

$$f_x(v_x,x) = \hbar\,\frac{s}{1+s}\,\delta k_{\rm L}\tan(k_{\rm L}x)\left\{1 + \frac{\gamma^2(1-s) - 2s^2[\delta^2 + (\gamma^2/4)]}{\gamma[\delta^2 + (\gamma^2/4)](1+s)^2}\,k_{\rm L} v_x \tan(k_{\rm L}x)\right\} \,, \tag{18.51}$$

where

$$s = \frac{8\Omega_0^2 \cos^2(k_L x)}{\delta^2 + (\gamma^2/4)} \,. \tag{18.52}$$

For weak intensities, the interference effects average to zero over a wavelength, hence the friction force averaged over a wavelength coincides with the sum of the two friction forces exerted by the two counterpropagating plane waves. In particular,

$$\bar{f} = -\alpha v \quad \text{with} \quad \alpha = -4\hbar k_L^2 \Omega_0^2 \frac{\delta\gamma}{[\delta^2 + (\gamma^2/4)]^2} \,. \tag{18.53}$$

Hence, because of the Doppler effect, for $\delta < 0$ the atom gets closer to resonance with the wave opposing its motion and further away from resonance with the other wave, so that the two forces exerted by the two waves become unbalanced and the net force opposes the motion of the atom. This is the mechanism for Doppler cooling.

18.4 Dressed State Description of the Dipole Force

If the Rabi frequency is large compared to the spontaneous emission rate the dressed atom picture provides an intuitive interpretation. We may write the interaction Hamiltonian for a two level atom, with frequency ω_a, interacting with a single mode standing wave laser field with frequency $\Omega_L = \omega_a + \Delta$

$$H_I(x) = \frac{\hbar\Delta}{2}\sigma_z + \hbar g(x)\left(a\sigma_+ + a^\dagger\sigma_-\right) \,, \tag{18.54}$$

where $g(x) = gf(x)$ is the spatially dependent vacuum Rabi frequency, $\sigma_+ = \sigma_-^\dagger = |e\rangle\langle g|$ and $a, a^\dagger$ are the annihilation and creation operators for the field. The dressed states (see section 10.2) for this interaction are:

$$|n,+\rangle = \sin\theta_n(x)|n,e\rangle + \cos\theta_n(x)|n+1,g\rangle \tag{18.55}$$

$$|n,-\rangle = \cos\theta_n(x)|n,e\rangle - \sin\theta_n(x)|n+1,g\rangle \tag{18.56}$$

where $|n,e\rangle = |n\rangle \otimes |e\rangle$, $|n,g\rangle = |n\rangle \otimes |g\rangle$ with $|n\rangle$ a photon number eigenstate. The coefficients are given by

$$\cos 2\theta_n(x) = -\frac{\Delta/2}{\Omega_n(x)} \,, \tag{18.57}$$

$$\sin 2\theta_n(x) = \frac{g(x)}{\Omega_n(x)} \,, \tag{18.58}$$

and $\Omega_n(x) = \sqrt{g^2(x)(n+1) + \Delta^2/4}$ is the effective Rabi frequency. The corresponding energy levels are $U_{n,\pm}(x) = \pm\hbar\Omega_n(x)$. This is a generalisation of the dressed state

picture discussed in Sect. 10.2. since the expansion coefficients are now position dependent. The dressed states form doublets separated the photon energy $\hbar\omega_L$.

Typically the optical field is well approximated by a coherent state of large amplitude. The Poisson nature of the photon number distribution in such a state enables us to replace $\Omega_n(x)$ by its average value $\Omega(x) = \sqrt{g^2 I(x) + \Delta^2/4}$ where $I(x) = f^2(x)\bar{n}$ and $\bar{n}$ is the average photon number is the field. Thus $I(x)$ is the spatially varying intensity of the field.

The variation in x of the energies of the dressed states are shown in Fig. 18.2 for two manifolds $\varepsilon(N)$ and $\varepsilon(N-1)$. The manifolds are connected by spontaneous emission. Outside the laser beam the energy levels of the dressed states tend to the uncoupled states and are separated by the detuning Δ. Within the laser beam $I(x)$ is nonzero and the splitting

$$\hbar\Omega(x) = \hbar\sqrt{4g^2 I(x) + \Delta^2} \tag{18.59}$$

between the two dressed levels of the same manifold increases with increasing values of $I(x)$.

We shall now use this dressed state picture to provide a physical description of the dipole force. Initially we shall neglect spontaneous emission. We assume the system is either in state $|n,+\rangle$ or $|n,-\rangle$ and satisfies the semiclassical limit (7). Assuming the atom velocity is sufficiently slow so that nonadiabatic transitions from one level to another can be neglected, the system will follow adiabatically the level $|n,+\rangle$ or $|n,-\rangle$ in which it is found initially. The energy curves in Fig. 18.2 are then potential energy level curves $V_{e,n}(x)$ and $V_{g,n}(x)$. The dressed atom therefore experiences a force

$$F_g = -\nabla V_{g,n}(x) = -\frac{\hbar}{2}\nabla\Omega(x)\,, \tag{18.60}$$

if it is in level $|g\rangle$ and a force

$$F_e = -\nabla V_{e,n}(x) = \frac{\hbar}{2}\nabla\Omega(x) = -F_g, \tag{18.61}$$

if it is in level $|e\rangle$.

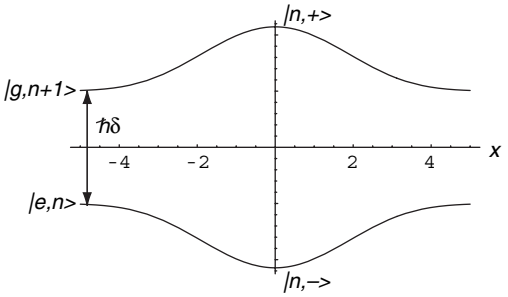

Fig. 18.2 The dependance of the dressed state energy levels on position due to a spatially varying intensity, a Gaussian beam profile

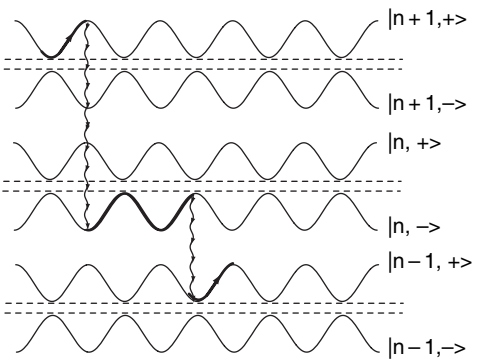

Fig. 18.3 A slow moving atom in a standing wave is cooled by spontaneous emission: Sisyphus cooling

This dependence of the force on the internal state is very similar to the Stern–Gerlach effect that occurs for a spin $\frac{1}{2}$ particle in an inhomogeneous magnetic field. This effect is known as the optical Stern–Gerlach effect will be described in more detail in Sect. 18.6. It also provides a mechanism for atom mirrors where atoms in one of the dressed states are repelled by a light field.

Spontaneous emission causes the dressed atom to make a transition to a lower manifold. In doing so it may change the type of state it is in e.g. a transition $|g,n+1>\rightarrow|g,n\rangle$ by emitting a photon. This causes the sign of the force to change abruptly. The time intervals τ_1 and τ_2 spent in the different dressed levels between two successive quantum jumps are Poisson random variables. This gives rise to the fluctuations in the dipole force.

The mean dipole force in the steady state is given by the mean of the forces F_1 and F_2 weighted by the proportion of time spent in the type 1 and 2 levels, which are simply the steady state populations of the dressed levels π_1 and π_2. Thus

$$\left\langle F_{\text{dip}}\right\rangle = F_1\pi_1 + F_2\pi_2 = -\frac{\hbar^2}{2}\nabla\Omega(x)(\pi_1-\pi_2)\ . \tag{18.62}$$

This corresponds to the expression derived earlier.

The dressed state picture gives a clear illustration of the mechanism for cooling a moving atom in a strong standing wave, known as Sisyphus cooling. In this case $I(x) = I_0\sin^2(k_L x)$. Figure 18.3 represents the dressed states for a positive detuning (blue detuning). The dressed states are linear combinations of ground and excited states, the weighting of which varies sinusoidally in space. If we follow an atom starting at the node of a standing wave in level $|g,n+1\rangle$, it climbs up the light gradient until it reaches the top (antinode) where its decay rate is a maximum as the mixed state has a significant excited state component. It may then jump into level $|g,n+1\rangle$ which does not effect its mechanical motion or jump into level $|e,n\rangle$ in which case the atom is again in a valley. It now must climb against the gradient to reach the top where it will decay by spontaneous emission again. The mechanism has been named Sisyphus cooling by analogy with the story from Greek mythology.

Between two spontaneous emissions, the total energy (kinetic plus potential) of the atom is conserved. When the atom climbs up hill, its kinetic energy is transformed into potential energy by stimulated emission processes which redistribute photons between the two counterpropagating waves at rate Ω. Atomic momentum is therefore transferred to laser photons. The total atomic energy is then dissipated by spontaneous emission which carries away part of the atomic potential energy. The force reaches its maximum value for velocities such that the atom travels over a distance of the order of a wavelength between two spontaneous emissions ($k_{\mathrm{L}} v_0 \sim \gamma$). The magnitude of this friction force is directly related to the modulated depth (Ω) of the dressed energy levels and hence increases indefinitely with laser intensity.

18.5 Atomic Diffraction by a Standing Wave

We shall consider the deflection of a beam of two-level atoms by a classical standing wave light field in a cavity. The atomic beam is normally incident on the standing wave and experiences an exchange of momentum with the photons in the light wave. We shall assume that the frequency of the light field is well detuned from the atomic resonance so that we may neglect spontaneous emission.

The Hamiltonian describing the interaction is

$$\mathscr{H} = \hbar\frac{\omega_0}{2}\sigma_z + \frac{\boldsymbol{p}^2}{2m} + \hbar\Omega(\sigma_- \mathrm{e}^{-\mathrm{i}\omega t} + \sigma_+ \mathrm{e}^{\mathrm{i}\omega t})\cos kx\,, \tag{18.63}$$

where $\boldsymbol{p}$ is the centre of mass momentum of the atom along the transverse (x direction), m is the atomic mass, σ_z and $\sigma_\pm$ are the pseudo spin operators for the atom, ω_0 and ω are the atomic and field frequencies, $k = \omega/c$ is the wave number of the standing wave, and $\Omega = \mu\varepsilon_0/\hbar$ the Rabi frequency with μ being the dipole moment and ε_0 the maximum field amplitude. We shall assume that the interaction time is sufficiently small that the transverse kinetic energy absorbed by the atom during the interaction can be neglected. This is known as the Raman–Nath regime and requires $t < 2\pi/\omega_r$, where the recoil energy is $\hbar\omega_r = (2r\hbar k)^2/2m$ where r is an integer. This is equivalent to neglecting the term $p^2/2m$ in the Hamiltonian.

Transforming to the interaction picture with $\mathscr{H}_0 = \hbar\omega\sigma_z$ the Hamiltonian may be written in the form

$$\mathscr{H} = \hbar\frac{\delta\omega}{2}\sigma_z + 2\hbar\Omega\sigma_x\cos kx\,, \tag{18.64}$$

where $\delta\omega = \omega_a - \omega$ and $2\sigma_x = \sigma_+ + \sigma_-$. This Hamiltonian may be diagonalised and written in the form

$$\mathscr{H} = V(x)[\cos\theta(x)\sigma_z + \sin\theta(x)\sigma_x] \tag{18.65}$$

where

$$V(x) = \hbar\sqrt{(\delta\omega)^2 + (2\Omega\cos kx)^2},$$
$$\cos\theta(x) = \frac{\delta\omega}{\sqrt{(\delta\omega)^2 + (2\Omega\cos kx)^2}},$$
$$\sin\theta(x) = \frac{2\Omega\cos kx}{\sqrt{(\delta\omega)^2 + (2\Omega\cos kx)^2}}.$$

In the limit of large detuning ($\delta\omega \gg 2\Omega\cos kx$),

$$\cos\theta \approx 1, \quad \text{and} \quad \sin\theta \approx 0,$$

so that

$$V(x) \approx \hbar\delta\omega\left(1 + \frac{2\Omega^2\cos^2 kx}{\delta\omega^2}\right). \tag{18.66}$$

This leads to the effective Hamiltonian

$$\mathscr{H}_{\text{eff}} = \hbar\frac{\delta\omega}{2}\sigma_z + \left(\frac{2\hbar\Omega^2\cos^2 kx}{\delta\omega}\right)\sigma_z. \tag{18.67}$$

The atomic state vector in the coordinate representation may be written as

$$\langle x|\psi(t)\rangle = a(x,t)|a\rangle + b(x,t)|b\rangle, \tag{18.68}$$

where $|a\rangle$ and $|b\rangle$ are the upper and lower atomic states, and $a(x,t)(b(x,t))$ are the probability amplitudes for the atom to be in the upper (lower) state at the transverse coordinate x at time t.

We assume that the atoms are initially in their ground state with a Gaussian wavefunction

$$a(\xi,0) = 0,$$
$$b(\xi,0) = (\pi\sigma^2)^{-1/4}\exp\left(-\frac{\xi^2}{2\sigma^2}\right), \tag{18.69}$$

where $\xi = kx$ and σ is proportional to the r.m.s. transverse position spread of the input beam. This may be written as

$$b(\xi,0) = \left(\frac{2\sigma_\eta^2}{\pi}\right)^{1/4}\exp[-(\sigma_\eta\xi)^2], \tag{18.70}$$

where σ_η is the r.m.s. transverse momentum spread of the input beam scaled to the photon momentum $\hbar k(\eta = p/\hbar k)$. The Schrödinger equation in the large detuning limit is

$$\frac{\partial}{\partial\tau}\begin{pmatrix} a \\ b \end{pmatrix} = \begin{pmatrix} -\mathrm{i}\Delta - \frac{\mathrm{i}\cos^2\xi}{2\Delta} & 0 \\ 0 & \mathrm{i}\Delta + \frac{\mathrm{i}\cos^2\xi}{2\Delta} \end{pmatrix}\begin{pmatrix} a \\ b \end{pmatrix} \tag{18.71}$$

where $\tau = \Omega t$ and $\Delta = \delta\omega/2\Omega$. We shall assume that the atom interacts with a field of constant amplitude for a time τ. The Rabi frequency is Ω.

The solution for $b(\varepsilon,\tau)$ may be written in the form [8]

$$b(\xi,\tau) = \exp\left[\mathrm{i}\left(\Delta + \frac{1}{4\Delta}\right)\tau\right] \sum_{n=-\infty}^{\infty} \mathrm{i}^n J_n\left(\frac{\tau}{4\Delta}\right) \exp(2\mathrm{i}n\xi) b(\xi,0)\,. \tag{18.72}$$

Taking the Fourier transform of this relationship shows the effect in momentum space is a convolution

$$\begin{aligned}\tilde{b}(\eta,\tau) &= \exp\left[\mathrm{i}\left(\Delta + \frac{1}{4\Delta}\right)\tau\right] \sum_{n=-\infty}^{\infty} \mathrm{i}^n J_n\left(\frac{\tau}{4\Delta}\right) \delta(\eta - 2n) * \tilde{b}(\eta,0) \\ &= \exp\left[\mathrm{i}\left(\Delta + \frac{1}{4\Delta}\right)\tau\right] \sum_{n=-\infty}^{\infty} \mathrm{i}^n J_n\left(\frac{\tau}{4\Delta}\right) \tilde{b}(\eta - 2n,0)\end{aligned} \tag{18.73}$$

where $\tilde{b}$ denotes the Fourier transform of b.

The scattered ground state wavefunction is a superposition of Gaussian modulated plane waves with momenta $p = 2n\hbar k$. The momentum transferred from the field to the atom is in even multiplies of $\hbar k$ corresponding to the absorption of a photon from the $(+k)$ component, followed by induced emission into the $(-k)$ component of the standing wave. The final output momentum probability distribution is composed of a comb of images of the initial momentum distribution. In order to resolve these peaks it is necessary to have a narrow initial momentum spread such that $\Delta p \ll 2\hbar k$ or $\sigma_\eta \ll 1$. The output momentum distribution is shown in Fig. 18.4 for $\sigma_\eta = 0.1$, where the propagation time after the interaction is assumed short so that further spreading has been neglected. The above result holds for large atomic detuning. For smaller atomic detunings spontaneous emission becomes important. Since the recoil imparted to an atom by a spontaneously emitted photon occurs in a random direction, exchanges of momentum in non-integral multiples of $\hbar k$ may occur and the diffractive peaks will be smeared out. That is, as the laser is tuned closer

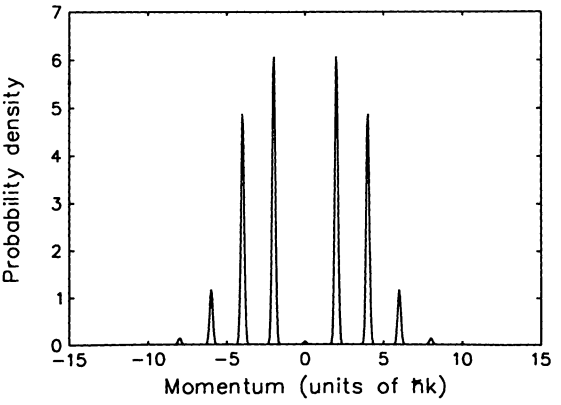

Fig. 18.4 Output momentum distribution for atoms scattered from a standing optical wave in the Kapitza-Dirac regime in the large detuning limit. Initial RMS momentum uncertainty is $\sigma_\eta = 0.1$ (units of $\hbar k$) and the normalised interaction time $\tau/\Delta = 10$

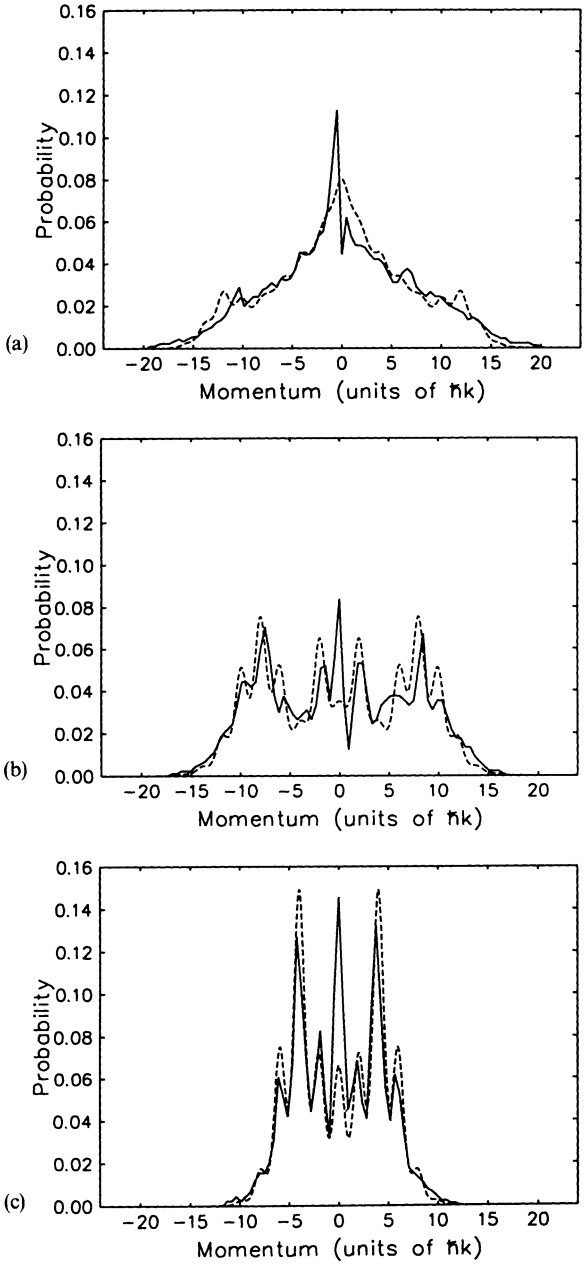

Fig. 18.5 Output momentum distribution for atoms scattered from a standing optical wave. Comparison of experimental data [20] (−) and theoretical predictions [21] (− − −) for (a) $\Delta = 0$, (b) $\Delta = 0.6$, (c) $\Delta = 1.2$ (from [10])

to the atomic resonance one moves from the diffractive to the diffusive regime. The transition from the diffractive to the diffusive regime has been demonstrated in an experiment by *Gould* et al. [11]. A fit to their data using a calculation which includes spontaneous emission has been given by *Tan* and *Walls* [10] and is shown in Fig. 18.5.

18.6 Optical Stern–Gerlach Effect

In the previous section, we discussed the diffraction of atoms in their ground state from a standing wave light field. In order to resolve the diffraction peaks in the momentum distribution it was necessary that the initial atomic spatial wave packet be larger than a wavelength. In this regime, the momentum transfer is symmetrical about $\Delta p = 0$ and is the same for input atoms in either the ground or excited states. As the spatial extent of the input wave packet is reduced to a fraction of the optical wavelength, the momentum transfer becomes asymmetrical and dependent upon the initial atomic state. Figure 18.6 shows the outgoing probability density of the atomic momentum for an initial atomic beam width $\sigma = 0.3$. The solid curve is for atoms in the ground state while the dotted curve is for the excited state.

In the limit when the spatial extent of the input wave packet is very small compared to the optical wavelength, an input beam is split into two beams depending on its atomic state. This is called the optical Stern–Gerlach limit in which the atom interacts with only a small part of the light wave ($\Delta x^{\mathrm{IN}} \ll 1/k$) and the individual photon exchanges are not resolvable ($\Delta p \gg \hbar k$). In the large-detuning limit the momentum transfer, which can be many times the photon momentum, depends on the intensity gradient of the optical field. An experimental demonstration of the optical Stern–Gerlach effect has been given by *Sleator* et al. [12] using a beam of metastable He atoms (Fig. 18.7).

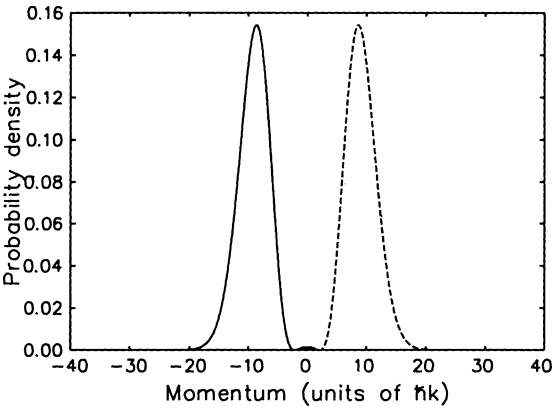

Fig. 18.6 Output momentum distribution for atoms scattered from a standing optical wave in the Stern-Gerlach regime. Initial rms momentum uncertainty is $\sigma_\eta = 2.4$ (units of $\hbar k$). The atomic beam is incident midway between a node and an antinode and the normalised interaction time $\tau/\Delta = 20$. (**a**) *solid curve*, ground state atoms, (**b**) *dotted curve*, excited state atoms

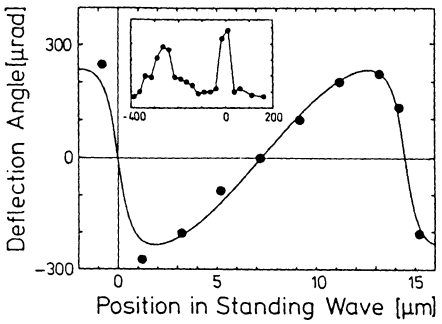

Fig. 18.7 Deflection of an atomic beam by a standing wave as a function of the atomic beam position in the standing wave. The detuning from resonance was $\Delta/2\pi = 160\,\mathrm{MHz}$. Position 0 on the horizontal scale was arbitrarily chosen to be at a node. Inset: Atomic intensity profile at the detector for the atomic beam at a position of $-11\,\mu\mathrm{m}$ in the standing wave. The peak at zero angle is due to undeflected atoms [12]

We shall demonstrate how the standing wave optical field encodes information about the atomic state in the centre of mass momenta of the outgoing atoms. A non-destructive determination of the atomic state may be useful in conjunction with micromaser experiments in which the photon statistics within the micromaser cavities are indirectly measured via their effects on the states of the Rydberg atoms which pass through them. The ability to spatially separate atoms according to their state without destroying them also makes it possible to consider their subsequent coherent recombination in an atomic interferometer.

In order to measure their atomic state we shall require that the momentum transfer be well correlated with the initial atomic state and that the process of splitting the input beam should not cause this atomic state to change. We shall demonstrate how one may make a QND measurement of the atomic inversion. We consider the case where the standing wave field is far detuned from the atomic resonance. In this case we may use the effective Hamiltonian given by (18.67).

The inversion of the atom, σ_z, we take as the signal observable and the centre of mass momentum p of the atom as the probe. It is evident that the Hamiltonian is back action evading for σ_z which is a constant of the motion. We shall follow the treatment given by *Tan* and *Walls* [13].

Consider a beam of atoms in a mixture of excited and ground states. The interaction with the standing light wave will impart some momentum to these atoms causing a deflection. The mean momentum transfer will have opposite signs for the two states. The mean momentum transfer compared to the standard deviation of the momentum transfer will determine how well the atomic beam can be separated into two beams of either excited or ground state atoms.

The probability amplitudes $a(\xi,\tau)$ and $b(\xi,\tau)$ for the atom to be in the excited and ground states at time τ are given in the large detuning limit by the solution of (18.71).

After passage through the field, the mean momentum transfer to this beam is given by

$$\langle \eta^{\mathrm{OUT}} \rangle = \int_{-\infty}^{\infty} a(\xi,\tau)^* \left(\frac{-\mathrm{i}\partial}{\partial \xi} \right) a(\xi,\tau)\mathrm{d}\xi + \int_{-\infty}^{\infty} b(\xi,\tau)^* \left(\frac{-\mathrm{i}\partial}{\partial \xi} \right) b(\xi,\tau)\mathrm{d}\xi \tag{18.74}$$

where $\eta = p/\hbar k$ is a normalised momentum. Similarly the mean squared momentum transfer is

$$\sigma_\eta^2 = \langle \eta^{\mathrm{OUT}^2} \rangle = \int_{-\infty}^{\infty} a^*(\xi,\tau) \left(\frac{-\partial^2}{\partial \xi^2} \right) a(\xi,\tau)\mathrm{d}\xi + \int b^*(\xi,\tau) \left(\frac{-\partial^2}{\partial \xi^2} \right) b(\xi,\tau)\mathrm{d}\xi \, . \tag{18.75}$$

In the large detuning limit we find for a Gaussian beam with width σ centred at ξ_0

$$\langle \eta_\pm^{\mathrm{OUT}} \rangle = \pm \frac{\tau}{2\Delta} \mathrm{e}^{-\sigma^2} \sin(2\xi_0) \tag{18.76}$$

$$\langle \eta_\pm^{\mathrm{OUT}^2} \rangle = \sigma_\eta^2 = \frac{1}{2\sigma^2} + \frac{\tau^2}{8\Delta^2} [1 - 2\mathrm{e}^{-2\sigma^2} \sin^2(2\xi_0) - \mathrm{e}^{-4\sigma^2} \cos(4\xi_0)] \tag{18.77}$$

where the $+$ sign is for initial state $|e\rangle$ and the $-$ sign for initial state $|g\rangle$. In Fig. 18.8 we plot these quantities as a function of the width of the atomic beam σ for $\tau/\Delta = 20$. The mean momentum transfer depends on the gradient of the intensity of the light field where the atom crosses and so the atomic beam must be narrow

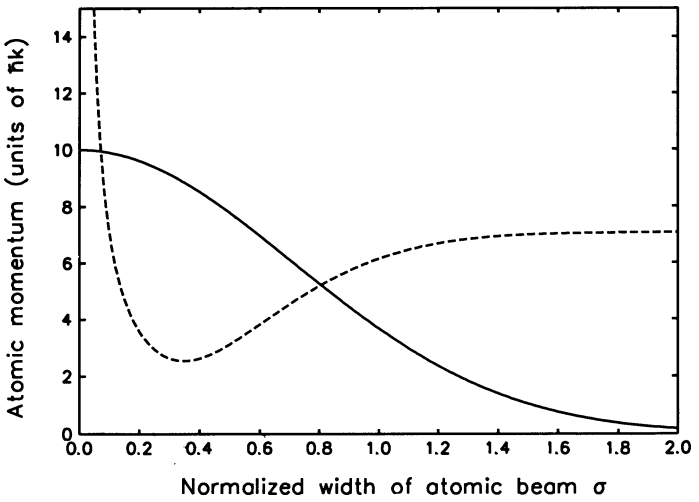

Fig. 18.8 Mean (*solid curve*) and standard deviation (*dashed curve*) of the atomic momentum plotted against the normalised width of the atomic beam. The atomic beam is incident midway between a node and an antinode and the normalised interaction time $\tau/\Delta = 20$ (from [13])

in order for the momentum transfer to be well defined. As the width of the atomic beam increases, different portions of the beam are deflected differently, reducing the mean momentum transfer. The variance of the output momentum arises from two effects: The term involving $(2\sigma^2)^{-1}$ represents the original momentum uncertainty of the input beam, which increases rapidly as σ is reduced. If, however, σ is increased so that it covers a significant portion of an optical wavelength, the variation in momentum imparted to different parts of the beam again increases the variance. Consequently there is a minimum in the standard deviation, as seen in Fig. 18.8. The condition for a good measurement is that the mean momentum transfer to the beam prepared in an eigenstate is larger than the spread of the outgoing momentum. From Fig. 18.8 it is clear that there is an optimal width of the input beam which gives the best quality of measurement. This optimum width depends on the interaction time since the mean momentum transfer rises with τ/Δ, and for larger interaction times this will exceed the intrinsic momentum uncertainty for a narrower initial beam. We may use the QND correlation coefficient introduced in Chap. 14 to evaluate the quality of the measurement. In this case the signal is the atomic inversion σ_z and the probe is the centre-of-mass momentum η of the atom.

These correlation coefficients depend on expectation values which have to be taken over some initial state. We choose the state which is a statistical mixture of ground and excited states with equal probability. In the large detuning limit the measurement correlation may be written as

$$C^2_{A_{\rm s}^{\rm IN}A_{\rm P}^{\rm OUT}} = \frac{|\langle \eta^{\rm OUT}\sigma_z^{\rm IN}\rangle|^2}{\langle \eta^{\rm OUT^2}\rangle\langle \sigma_z^{\rm IN^2}\rangle}$$

$$= \frac{|\frac{1}{2}[\langle \eta_+^{\rm OUT}\rangle(\frac{1}{2}) - \langle \eta_-^{\rm OUT}\rangle(\frac{-1}{2})]|^2}{\frac{1}{2}(\langle \eta_+^{\rm OUT^2}\rangle + \langle \eta_-^{\rm OUT^2}\rangle)\frac{1}{2}[(\frac{1}{2})^2 + (\frac{-1}{2})^2]}\,, \tag{18.78}$$

from (18.76 and 18.77) this may be written as

$$C^2_{A_{\rm s}^{\rm IN}A_{\rm P}^{\rm OUT}} = \frac{2\sigma^2\tau^2 {\rm e}^{-2\sigma^2}\sin^2(2\xi_0)}{4\Delta^2 + \sigma^2\tau^2[1 - {\rm e}^{-4\sigma^2}\cos(4\xi_0)]}\,. \tag{18.79}$$

The state preparation correlation $C^2_{A_{\rm s}^{\rm IN}A_{\rm P}^{\rm OUT}}$ has an identical expression. In the large detuning limit an atom prepared in an eigenstate of σ_z remains in an eigenstate of σ_z. Consequently, the non-demolition correlation

$$C^2_{A_{\rm s}^{\rm IN}A_{\rm s}^{\rm OUT}} = 1\,. \tag{18.80}$$

In Fig. 18.9 we plot $C^2_{A_{\rm s}^{\rm IN}A_{\rm P}^{\rm OUT}}$ as a function of the width of the atomic beam σ for a range of different interaction times $\tau/\Delta = 2, 5, 10, 20, 50$.

The position of the beam centre is $\xi_0 = \pi/4$ corresponding to the point midway between a node and antinode where the intensity gradient is greatest. We see that for sufficiently large interaction times and an atomic beam of optimal width the

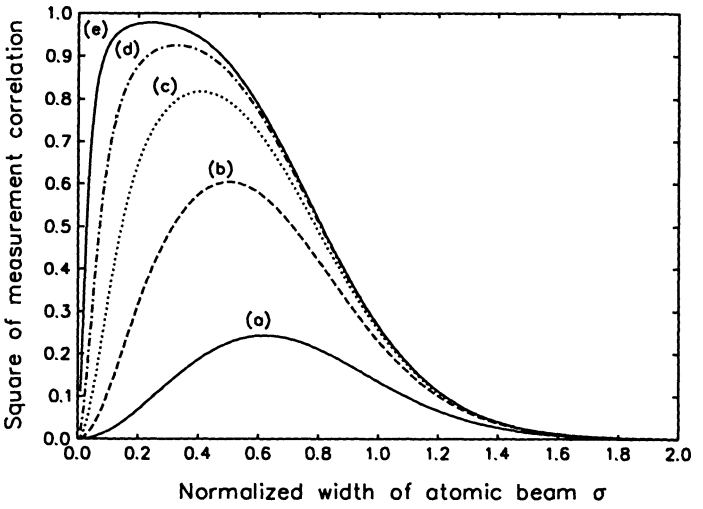

Fig. 18.9 Measurement correlation coefficient squared *plotted* against the normalised width of the atomic beam for $\tau/\Delta =$ (a) 2, (b) 5, (c) 10, (d) 20, (e) 50 (from [13])

measurement correlation may approach unity. Thus the deflection of an atomic beam by a standing wave field may be used to give a good QND measurement of the atomic inversion σ_z in the detuning limit. For smaller detuning a QND measurement of an operator $\mathrm{d}x\sigma_x + \mathrm{d}y\sigma_y + \mathrm{d}z\sigma_z$ can be made. For example, for zero detuning the appropriate QND observable is the atomic polarisation σ_x.

18.7 Quantum Chaos

A cold atom moving in a well detuned laser field sees a dipole potential that has the same spatial dependence as the field intensity. These potentials are usually non linear and anharmonic. They thus provide an ideal means to investigate anharmonic quantum non linear dynamics. Given the ease with which the optical field can be modulated in time, we also have the possibility of investigating non adiabatic dynamics of time dependent potentials and quantum chaos.

We can describe both spatial and temporal modulation through the Rabi frequency $\Omega(x,t)$. As we have seen a two-level atom moving in one dimension (the x-direction) in an off-resonant field can be well described by the effective Hamiltonian

$$H_{\mathrm{eff}} = \frac{p_x^2}{2m} + \frac{|\Omega(x,t)|^2}{2\Delta}\sigma_z \tag{18.81}$$

where $\Delta = \omega_{\mathrm{L}} - \omega_a$. We will typically be concerned with a standing wave laser field with wave vector k, with modulated intensity. In that case

$$\Omega(x,t) = \Omega[1 - 2\varepsilon\cos(\omega\tau)]\sin(kx) \tag{18.82}$$

Following [14] we introduce dimensionless variables for convenience:

$$\bar{\hbar} = \frac{4\hbar k^2}{m\omega} \tag{18.83}$$

$$\kappa = \frac{\hbar k^2 \Omega^2}{2m\omega^2\Delta} \tag{18.84}$$

$$t = \omega\tau \tag{18.85}$$

$$q = 2kx \tag{18.86}$$

$$p = \frac{2kp_x}{m\omega} \tag{18.87}$$

Noting that the commutation relation for the dimensionless position and momentum is

$$[q,p] = \mathrm{i}\bar{\hbar} \tag{18.88}$$

we see that $\bar{\hbar}$ has the interpretation of a dimensionless Planck's constant.

We first consider the case of a time independent standing wave. In this case the Hamiltonian in dimensionless variables is

$$H = \frac{p^2}{2} - \kappa\cos q \tag{18.89}$$

This is a standard problem in classical nonlinear dynamics and is fully integrable by a canonical transformation to action-angle variables. If at time $t = 0$ the atom has initial conditions $(q(t=0), p(t=0)) = (q_0, p_0)$ it will move in the phase space so as to conserve energy so it must remain on the curve $E = p(t)^2/2 - \kappa\cos(q(t)) = p_0^2/2 - \kappa\cos(q_0)$. The motion is periodic if the initial energy is such that $-\kappa < E < 0$, in which case the atom remains localised in one well. For $E > \kappa$ the motion is unbounded. The curve $E = 0$ is called the spearatrix. The frequency of the oscillatory motion depends on energy, and tends to zero as the initial energy approaches zero on the separatrix. This is shown in Fig. 18.10.

The nonlinear dependance of oscillator frequency on energy is important when we add a periodic temporal modulation to the potential. For a simple harmonic oscillator, resonance is only possible at one frequency and this does not depend on initial conditions. For a non linear oscillator this is no longer the case and a complex hierarchy of resonances is possible leading to chaos. In fact, periodically driven systems with a nonlinear potential is generically chaotic even in one dimension. Consider the case of an atom in a standing wave with modulated amplitude. The Hamiltonian is

$$H(t) = \frac{p^2}{2} - \kappa(1 - 2\varepsilon\cos t)\cos q \tag{18.90}$$

As the Hamiltonian is periodic in time, the most appropriate way to describe the dynamics is in terms of a Poincaré section with respect to time. This means that we

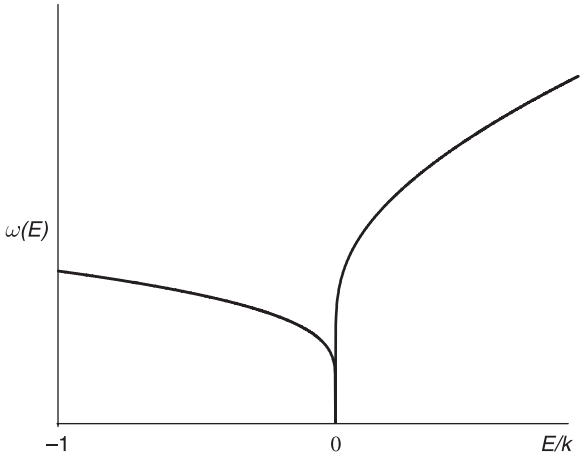

Fig. 18.10 The energy dependance of the oscillation frequency for an atom moving in a sinusoidal potential, $\omega(E)$ versus E/κ. Note that for energies at the bottom of the wells, the energy is almost independent of frequency, and the motion is simple harmonic

only need to view the dynamics at discrete times which are multiples of the driving period (see [15]). This defines a non linear map on phase space which is sometimes called a *stroboscopic map*. In figure 18.11 we illustrate this for a variety of initial conditions. A number of islands of regular motion are apparent surrounded by a sea of chaotic orbits.

18.7.1 Dynamical Tunnelling

The regular orbits are near elliptic fixed points of period-one of the map. The two inner regular orbits apparent in Fig. 18.11 are two distinct period-one orbits. If the system is prepared with initial conditions close to one of these period-one orbits it must remain within the island of stability surrounding the fixed point. A distribution of phase space points initially localised in this region will remain localised. As we now discuss, this is no longer the case quantum mechanically.

The quantum equivalent of a stroboscopic map is the unitary operator corresponding to the dynamics integrated over one period of modulation. This is called the Floquet operator, $\hat{F}$. Iterations of the quantum map are thus defined by

$$|\psi_{n+1}\rangle = \hat{F}|\psi_n\rangle \tag{18.91}$$

As the dynamics is not integrable even classically the operator $\hat{F}$ is difficult find and we must resort to numerical methods. See [16] for further discussion. Once it is found, we proceed by first finding its eigenstates and eigenvalues (which must all lie on the unit circle)

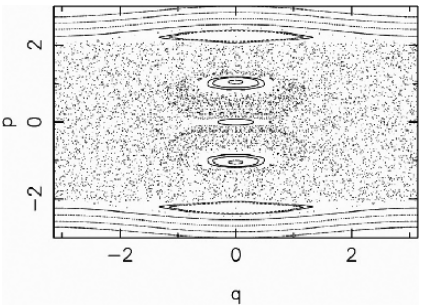

Fig. 18.11 The classical phase space orbits for the stroboscopic map with a variety of initial conditions. The modulation strength is $\varepsilon = 0.3$

$$\hat{F}|\phi_\alpha\rangle = \mathrm{e}^{\mathrm{i}\phi_\alpha}|\phi_\alpha\rangle \tag{18.92}$$

It is a remarkable fact that the eigenstates can often be put in one to one correspondence with particular orbits of the classical map, using a phase space representation such as the Q-function. For example there are pair of nearly degenerate eigenstates associated with the period one fixed points near the origin in Fig. 18.11. Given the solution to the eigenvalue problem the iteration of a given initial state is found by expanding the state over the Floquet eigenstates, $|\psi_0\rangle = \sum_\alpha c_\alpha |\phi_\alpha\rangle$

$$|\psi_n\rangle = \sum_\alpha c_\alpha \mathrm{e}^{\mathrm{i}n\phi_\alpha}|\phi_\alpha\rangle \tag{18.93}$$

We now take the initial state to be well localised inside the island of stability surrounding one of the period one orbits. We iterate the state and at each iteration step calculate the average and variance of the position and momentum. The results are plotted in Fig. 18.12. We see a very different situation to what would be expected classically (also shown in the figure). The quantum state does not remain localised near the period one fixed point at which it started. Rather it appears to tunnel across classically forbidden regions of phase space to the symmetric partner of the fixed

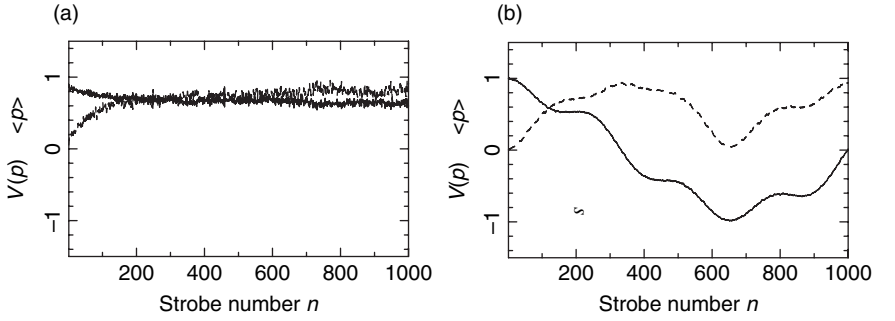

Fig. 18.12 The average and variance of position and momentum for an initial classical distribution (**a**) localised near a period one fixed point and (**b**) an initial quantum state localised near a period one fixed point. The quantum system demonstrates tunneling form one period one fixed point to another

point. This is called dynamical tunneling [17]. Dynamical tunneling was observed by *Hensinger* et al. [18] using a Bose Einstein condensate to prepare the initial localised state in phase space.

18.7.2 Dynamical Localisation

More complicated anharmonic modulation of the optical dipole potential can be easily implemented. An extreme case corresponds to a kicked system in which the standing wave is pulsed on and off very quickly compared to the period of free dynamics between pulses. In the limit of infinitely short pulses we obtain the delta kicked rotor described by the Hamiltonian

$$H(t) = \frac{p^2}{2} - \kappa \cos q \sum_n \delta(t-n) \tag{18.94}$$

This is a well studied system that classically is described by a stroboscopic map that is an example of the *standard map*. If the kicking strength, κ, is sufficiently large the phase space is dominated by large sea of chaotic orbits. In this region an initial well localised distribution of points spreads very rapidly in position but only slowly diffuses in momentum. In fact to a very good approximation the spread in momentum is indeed described by a diffusion process with diffusion constant proportional to κ. See [19] for further detail.

The quantum description of this system gives a very different result. An initial state well localised in momentum will follow the classical diffusion until a time know as the *break time*. At that time the diffusion in momentum will cease and the momentum variance saturates. This is illustrated in Fig. 18.13. Dynamical localisation using laser cooled atoms was first observed by Raizen's group in 1995 [20].

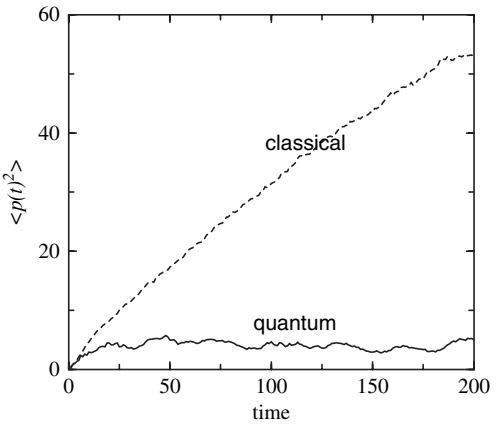

Fig. 18.13 Classical *(dashed)* and quantum *(solid)* of the average momentum squared versus kick number. In this example $\hbar = 0.24, \kappa = 1.2$

18.8 The Effect of Spontaneous Emission

In this section we give a brief presentation of the effect of spontaneous emission on the nonlinear quantum dynamics of atoms. Even in a far detuned optical dipole potential there is a non zero probability that the atom will be excited. In that case it suffers a recoil induced momentum kick. Once in the excited state it can relax to the ground state by either stimulated emission or spontaneous emission. The best way to deal with the stochastic momentum kicks resulting from absorption, or stimulated and spontaneous emission is via the stochastic Schrödinger equation discussed in Chap. 6.

We will follow the approach of Dyrting [21]. The coherent coupling between the internal and center-of-mass variables is through the position dependent Rabi frequency. We can write the Rabi frequency in the general form

$$\Omega(x) = \Omega f(kx,t) \,. \tag{18.95}$$

$k = c/\omega_{\mathrm{L}}$ is called the wavenumber and ω_{L} is the frequency of the laser. Ω is a measure of the intensity of the field and without loss of generality it can be chosen to be real and may be explicitly time dependent. The quantum mechanical atom can be described by its internal state $|\sigma\rangle$, where σ represents either g or e, and a centre-of-mass state $|\psi\rangle$.

The master equation for a two-level atom interacting with the field including spontaneous emission is

$$\frac{\mathrm{d}\hat{R}}{\mathrm{d}\tau} = -\frac{\mathrm{i}}{\hbar}\left[\hat{H},\hat{R}\right] - \gamma\mathscr{L}\hat{R} \,. \tag{18.96}$$

The Hamiltonian $\hat{H}$ generates the coherent dynamics for the center-of-mass and internal states of the atom. The superoperator $\mathscr{L}$ describes incoherent evolution due to coupling with the vacuum field modes at a rate γ. The effect of a spontaneous emission causes the atom to make a transition from its internal excited state to its ground state, and the spontaneously emitted photon changes its center-of-mass momentum by an amount $\hbar k\mathbf{n}$. The direction of the emitted photon $\mathbf{n}$ is random and has the distribution function

$$\phi(\mathbf{n}) = \frac{3}{8\pi}\left(1 - \frac{(\mathbf{d}\cdot\mathbf{n})^2}{\mathbf{d}\cdot\mathbf{d}}\right) \,. \tag{18.97}$$

$\mathscr{L}$ is given by

$$\mathscr{L}\hat{R} = \frac{1}{2}\left(\hat{\sigma}^\dagger\hat{\sigma}\hat{R} + \hat{R}\hat{\sigma}^\dagger\hat{\sigma} - 2\hat{\sigma}\mathscr{N}\hat{R}\hat{\sigma}^\dagger\right) \,, \tag{18.98}$$

and $\mathscr{N}$ is the superoperator describing the effect of a spontaneous emission on the transverse momentum of the atom

$$\mathscr{N}\hat{R} = \int \phi(\mathbf{n}) \exp\left(\mathrm{i}\mathbf{n}k\hat{x}\right)\hat{R}\exp\left(-\mathrm{i}\mathbf{n}k\hat{x}\right) d\mathbf{n} \,. \tag{18.99}$$

Here the integral is done over the surface of the unit sphere $\mathbf{n}\cdot\mathbf{n}=1$.

In the limit that the detuning Δ is much larger than the Rabi frequency Ω and the spontaneous emission rate γ the system can be described by the effective master equation

$$\frac{\mathrm{d}\hat{R}}{\mathrm{d}\tau} = -\frac{\mathrm{i}}{\hbar}\left[\hat{H}_0,\hat{R}\right] - \gamma\mathscr{L}\hat{R} + \frac{\mathrm{i}}{\Delta}\left[\Omega(\hat{x})\hat{\sigma}^\dagger, \left(1-\mathrm{i}\frac{\gamma}{\Delta}\mathscr{L}\right)^{-1}\left[\Omega(\hat{x})^\dagger\hat{\sigma},\hat{R}\right]\right] - \frac{\mathrm{i}}{\Delta}\left[\Omega(\hat{x})^\dagger\hat{\sigma}, \left(1+\mathrm{i}\frac{\gamma}{\Delta}\mathscr{L}\right)^{-1}\left[\Omega(\hat{x})\hat{\sigma}^\dagger,\hat{R}\right]\right], \tag{18.100}$$

where $\hat{H}_0$. The evolution of the reduced center-of-mass density operators $\hat{\rho}_g = \langle g|\hat{R}|g\rangle$ and $\hat{\rho}_e = \langle e|\hat{R}|e\rangle$ is given by the coupled equations

$$\frac{\mathrm{d}\hat{\rho}_g}{\mathrm{d}t} = -\frac{\mathrm{i}}{\bar{k}}\left[\hat{H}_g,\hat{\rho}_g\right] + \Gamma\mathscr{N}\hat{\rho}_e - \frac{\eta}{2}\left[\left\{f(\hat{q}/2,t)^\dagger f(\hat{q}/2,t),\hat{\rho}_g\right\} - 2f(\hat{q}/2,t)^\dagger\hat{\rho}_e f(\hat{q}/2,t)\right], \tag{18.101}$$

$$\frac{\mathrm{d}\hat{\rho}_e}{\mathrm{d}t} = -\frac{\mathrm{i}}{\bar{k}}\left[\hat{H}_e,\hat{\rho}_e\right] - \Gamma\hat{\rho}_e - \frac{\eta}{2}\left[\left\{f(\hat{q}/2,t)^\dagger f(\hat{q}/2,t),\hat{\rho}_e\right\} - 2f(\hat{q}/2,t)\hat{\rho}_g f(\hat{q}/2,t)^\dagger\right], \tag{18.102}$$

where

$$\hat{H}_g = \frac{\hat{p}^2}{2} + \frac{2\kappa}{|\nu|^2}f(\hat{q}2,t)^\dagger f(\hat{q}/2,t), \tag{18.103}$$

$$\hat{H}_e = \frac{\hat{p}^2}{2} - \frac{2\kappa}{|\nu|^2}f(\hat{q}/2,t)^\dagger f(\hat{q}/2,t), \tag{18.104}$$

and $\nu = 1-\mathrm{i}\gamma/2\Delta$ and $\{\ ,\ \}$ denotes the anti-commutator. We have again used the dimensionless variables for convenience: $\bar{k} = \frac{4\hbar k^2}{m\omega}$, $\kappa = \frac{\hbar k^2\Omega^2}{2m\omega^2\Delta}$, $\Gamma = \frac{\gamma}{\omega}$, $t = \omega\tau$, $\eta = \frac{\gamma\Omega^2}{4\omega\Delta^2|\nu|^2}$, $q = 2kx$, and $p = \frac{2kp_x}{m\omega}$.

The master equation may be unravelled as a stochastic Schrödinger equation as follows. The internal state changes according to the two jump processes N_1, and N_2 which have the following actions:

$$g \overset{N_1}{\to} e, \quad \text{absorption} \tag{18.105}$$

$$e \overset{N_1}{\to} g, \quad \text{stimulated emission} \tag{18.106}$$

$$g \overset{N_2}{\to} e \quad \text{spontaneous emission}. \tag{18.107}$$

These two jump processes proceed at the rates

$$E\left[\mathrm{d}N_1\right] = \eta\langle\psi|f(\hat{q}/2,t)^2|\psi\rangle\mathrm{d}t\ , \tag{18.108}$$

$$E\left[\mathrm{d}N_2\right] = \Gamma\mathrm{d}t\ . \tag{18.109}$$

Here $E[\,]$ denotes an ensemble average. thus represents spontaneous emission while $N_2(t)$ represents stimulated emission. The centre-of-mass state evolves according to the un-normalised stochastic Schrödinger equation

$$\mathrm{d}|\psi\rangle = -\frac{\mathrm{i}}{\hbar}\mathrm{d}t\hat{K}_\sigma|\psi\rangle + dN_1\left(\frac{f(\hat{q}/2,t)}{\sqrt{\langle f(\hat{q}/2,t)^2\rangle}} - 1\right)|\psi\rangle$$

$$+\,\mathrm{d}N_2\left(\frac{\exp\left(\mathrm{i}\bar{p}\hat{q}/\hbar\right)}{\sqrt{\langle\psi|\psi\rangle}} - 1\right)|\psi\rangle\ , \tag{18.110}$$

where $\langle f(\hat{q}/2,t)^2\rangle = \langle\psi|f(\hat{q}/2,t)^2|\psi\rangle$. This equation does not preserve the normalisation of the state $|\psi\rangle$. This will be important when we come to generate the times for the jump N_1. The jump terms determine the state after a jump $|\psi_{\text{after}}\rangle$ in terms of the state before $|\psi_{\text{before}}\rangle$ by

$$N_1:\ |\psi_{\text{after}}\rangle = \frac{f(\hat{q}/2,t)|\psi_{\text{before}}\rangle}{\sqrt{\langle\psi_{\text{before}}|f(\hat{q}/2,t)^2|\psi_{\text{before}}\rangle}}, \tag{18.111}$$

$$N_2:\ |\psi_{\text{after}}\rangle = \frac{\exp\left(\mathrm{i}\bar{p}\hat{q}/\hbar\right)|\psi_{\text{before}}\rangle}{\sqrt{\langle\psi_{\text{before}}|\psi_{\text{before}}\rangle}}\ . \tag{18.112}$$

where $\bar{p}$ is the random kick in momentum due to spontaneous recoil which satisfies

$$\text{Prob}(\bar{p},\bar{p}+\mathrm{d}\bar{p}) = \phi(\bar{p})\mathrm{d}\bar{p} \tag{18.113}$$

The operator $\hat{K}_\sigma$ is non-Hermitian and depends on the internal state σ as follows:

$$\hat{K}_\sigma = \begin{cases} \hat{p}^2/2 + V(\hat{q},t)/\nu^* & \sigma = g \\ \hat{p}^2/2 - V(\hat{q},t)/\nu & \sigma = e. \end{cases} \tag{18.114}$$

where $\nu = 1 - \mathrm{i}\gamma/2\Delta$ and $V(\hat{q},t) = f^\dagger(\hat{q},t)f(\hat{q},t)$. Between jumps the state evolves in a complex potential and the imaginary part of the complex potential causes the normalisation of $|\psi\rangle$ to decay. The effect of an N_1 jump is to change the internal state and to change the centre-of-mass state. The cumulative distribution function for the stimulated jump N_1 is given by

$$P_{\text{stim}}(t) = 1 - |\langle\psi(t)|\psi(t)\rangle|\ . \tag{18.115}$$

We generate a random number z_{stim} which has a uniform distribution on the interval and provided no spontaneous emission has occurred in the meantime we integrate the wave equation with generator $\hat{K}_\sigma$ to the time t such that $z_{\text{stim}} = 1 - |\langle\psi(t)|\psi(t)\rangle|$. In this way we compute when an atom makes a stimulated transition.

When the atom makes a transition to state b it is easy to generate the random number t_{spont} equal to the time the atom spontaneously emits using the cumulative distribution function $P_{\text{spont}}(t) = 1 - \exp(-\Gamma t)$. The effect of spontaneous emission N_2 is to change the momentum of the state by the amount $\bar{p}$ given by

$$\bar{p} = \hbar k \left(\cos\zeta \cos\theta + \sin\phi \sin\theta \sin\zeta\right)/2 \,, \tag{18.116}$$

where ζ is the angle between the dipole moment and the x-axis. The angle $\phi \in [0, 2\pi]$ is random with a uniform distribution and θ is given by

$$\theta = \arccos\left[2\cos\left(\frac{\arccos(2y-1)+4\pi}{3}\right)\right] \,, \tag{18.117}$$

where $y \in [0,1]$ is a random number with a uniform distribution. In our numerical calculations we have chosen $\zeta = \pi/2$.

To recover the centre-of-mass density operator one takes the ensemble average of the conditioned operators

$$\hat{\rho} = \hat{\rho}_g + \hat{\rho}_e = E\left[\frac{|\psi\rangle\langle\psi|}{\langle\psi|\psi\rangle}\right] \tag{18.118}$$

In the simulations of [16] the state $|\psi\rangle$ was evolved forward for a time δt using the first order split operator method. Then the norm of $|\psi(t+\delta t)\rangle$ is calculated to determine if a stimulated jump has occurred and whether the spontaneous emission time t_{spont} is reached. If a jump occurs the appropriate transformation (18.8) is

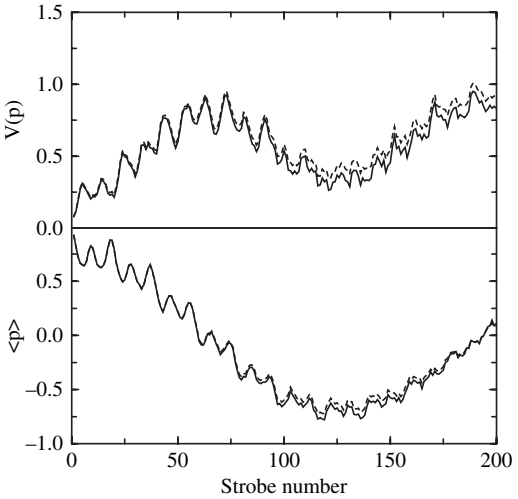

Fig. 18.14 Tunneling between second order resonances as reflected in the momentum mean $\langle p\rangle$ and variance $V(p)$. Solid line, coherent motion; dashed line with spontaneous emission included and $\Gamma = 1.525, \eta = 6.1 \times 10^{-}4$

applied in the momentum representation and then the new state is evolved forward δt and so on until it has been evolved forward the desired time. The whole process is repeated over 1,000 trajectories.

To test whether spontaneous emission obscures coherent tunneling simulations were made using the atomic system of Ytterbium with $\bar{k} = 0.25$ and with an initial wavepacket localised in phase space at $(q_0, p_0) = (0.0, 1.0)$ and a momentum variance of $V(p) = 0.04$. In Fig. 18.14 we show quantum Monte Carlo simulations with and without spontaneous emission. We still see definite sign of coherent tunneling even when spontaneous emission is included.

For the initial state a semi-classical an estimate, based on the simulation, for the coherence damping rate gives $\Gamma_{\rm coh} \approx 0.06\eta$. The time taken to tunnel to the opposite second order resonance is $T \approx 125 \times 2\pi$. This implies that the value $\eta \approx 0.02$ is required for the critical damping of the tunneling oscillations. Dynamic localisation is a coherent effect and noise due to spontaneous emission must be kept low. For the spontaneous decay rate of Ytterbium of $\gamma/2\pi = 183$ kHz, the spontaneous and stimulated rates are $\Gamma = 1.5$ and $\eta = 4.5 \times 10^{-4}$ respectively.

References

1. T.W. Hänsch, A.L. Schawlow: Opt. Comm. **13**, 68 (1975)
2. S. Chu, L. Hollberg, J.E. Bjorkholm, A. Cable, A. Ashkin: Phys. Rev. Lett. **55**, 48 (1985)
3. P.D. Lett, R.N. Watts, C.I. Westbrook, W.D. Phillips, P.L. Gould, H.J. Metcalf: Phys. Rev. Lett. **62**, 1118 (1988)
4. J. Dalibard, C. Cohen-Tannoudji: JOSA B**6**, 2023 (1989)
5. P.J. Ungar, D.S. Weiss, E. Ris, S. Chu: JOSA B**6**, 2058 (1989)
6. J. Gordon, A. Ashkin: Phys. Rev. A **21**, 1606 (1980)
7. C. Cohen-Tannoudji: Atomic Motion in Laser Light, in *Fundamental Systems in Quantum Optics*, edited by J. Dalibard et al. (Elsevier Science Publishers, 1991)
8. E.M. Wright, P. Meystre: Opt. Commun. **75**, 388 (1990)
9. T. Sleator, O. Carnal, A. Faulstich, J. Mlynek: In *Quantum Measurement in Optics*, edi. by P. Tombesi, D.F. Walls (Plenum, New York 1992)
10. S.M. Tan, D.F. Walls: Appl. Phys. B **54**, 434 (1992)
11. P.L. Gould, P.J. Martin, G.A. Ruff, R.E. Stoner, J.L. Pieque, D.E. Pritchard: Phys. Rev. A **43**, 585 (1991)
12. T. Sleator, T. Pfau, V. Balykin, O. Carnal, J. Mlynek: Phys. Rev. Lett. **68**, 1996 (1992)
13. S.M. Tan, D.F. Walls: Phys. Rev. A **47**, 663 (1993)
14. R.Graham, M. Schlautman, P. Zoller: Phys. Rev. A, **45**, R19, (1992)
15. L. Reichl: *The Transition to Chaos, in Conservative Classical Systems: Quantum Manifestations* (Springer Verlag, New York 1992)
16. S. Dyrting, G.J. Milburn, C.A. Holmes: Phys. Rev. E 48, 969–978 (1993)
17. M.J. Davis, E.J. Heller: Quantum Dynamical Tunneling in Bound States: J. Chem. Phys. **75**, 246 (1981)
18. W.K. Hensinger, H. Hffner, A. Browaeys, N.R. Heckenberg, K. Helmerson, C. McKenzie, G.J. Milburn, W.D. Phillips, S.L. Rolston, H. Rubinsztein-Dunlop, B. Upcroft: Nature, **412**, 52–55 (2001)
19. H.-J. Stöckman: *Quantum Chaos: An Introduction* (Cambridge University Press, 2001)
20. F.L. Moore, J.C. Robinson, C.F. Barucha, B. Sunduram, M.G. Raizen: Phys. Rev. Lett. **75**, 4598 (1995)

21. S. Dyrting, G.J. Milburn: Phys. Rev. A **51**, 3136 (1995)
22. T. Dittrich, R. Graham: Ann. Phys. **200**, 363 (1990)

Further Reading

S. Chu: Laser Manipulation of Atoms and Particles, Science **253**, 861 (1991)
E. Arimondo, W.D. Phillips, F. Strumia: *Laser Manipulation of Atoms and Ions* (North Holland, 1991)
H.J. Metcalf, P. van der Stratten: *Laser Cooling and Trapping* (Springer, New York 1999)
P. Meystre: *Atom Optics* (Springer, New York, 2001)
A.P. Kazantsev, G.I. Surdutovich, V.P. Yakovlev: *Mechanical Action of Light on Atoms* (World Scientific, 1990)